SEPTEMBER 2018 M.Sc. in Civil Engineering OMAR ALI ALHETE

UNIVERSITY OF GAZIANTEP
GRADUATE SCHOOL OF
NATURAL & APPLIED SCIENCES

EFFECTS OF IMPERFECTIONS ON THE FLEXURAL BEHAVIOUR OF CONCRETE FILLED STEEL TUBES BEAMS WITH CIRCULAR SECTIONS

M. Sc. THESIS
IN
CIVIL ENGINEERING

BY
Omar Ali ALHETE

SEPTEMBER 2018

Effects of Imperfections on the Flexural Behavior of Concrete Filled Steel Tubes Beams with Circular Sections

M.Sc. Thesis
In
Civil Engineering
University of Gaziantep

Supervisor
Asst. Prof. Dr. Mehmet Tolga GÖĞÜŞ

by

Omar Ali ALHETE

September 2018

REPUBLIC OF TURKEY
UNIVERSITY OF GAZİANTEP
GRADUATE SCHOOL OF NATURAL & APPLIED SCIENCES
CIVIL ENGINEERING

Name of the thesis: Concrete Fılled Steel Tube Beams With Square Sections: Effect Of Notches On The Flexural Performance.

Name of the student: Mohammed Muneam MOHAMMED

Exam date: 28.09.2018

Approval of the Graduate School of Natural and Applied Sciences

Prof. Dr. Ahmet Necmeddin YAZICI
Director

I certify that this thesis satisfies all the requirements as a thesis for the degree of Master of Science.

Prof. Dr. Hanifi ÇANAKÇI
Head of Department

This is to certify that we have read this thesis and that in our consensus opinion it is fully adequate, in scope and quality, as a thesis for of the degree of consensus or majority Master of Science.

Asst. Prof. Dr. Mehmet Tolga GÖĞÜŞ
Supervisor

Examining Committee Members:	Signature
Assist. Prof. Dr. Ahmet Emin KURTOĞLU	....
Assist. Prof. Dr. Mehmet Eren GÜLŞAN	....
Assist. Prof. Dr. M. Tolga GÖĞÜŞ	....

I hereby declare that all information in this document has obtained and presented in accordance with academic rules and ethical conduct. I also declare that, as required by these rules and conduct, I have fully cited and referenced all material and results that are not original to this work.

Omar Ali ALHETE

`

ABSTRACT

EFFECTS OF IMPERFECTIONS ON THE FLEXURAL BEHAVIOUR OF CONCRETE FILLED STEEL TUBES BEAMS CIRCULAR SECTIONS

ALHETE, Omar Ali
M.Sc. in Civil Engineering
Supervisor: Asst. Prof. Dr. Mehmet Tolga GÖĞÜŞ

September 2018
54 pages

Bending tests of the Concrete Filled Steel Tube (CFST) beams with artificial notches in the steel tubes were conducted in this thesis to investigate the effects of the material imperfections of steel tubes on beam flexural. This study presents the results of an experimental program the bending behaviors of CFST beams with notches in the steel tube circular two different thickness (2mm, 4mm) involve of 26 specimens which consist of 24 with notch CFST beams, two (control) without notch CFST beams were investigated in the present work. Investigating the flexural performance of Self-Compacting Concrete (SCC) filled steel tube beams The CFST with notches from the top, bottom and sidewall with two different thicknesses and two different lengths of the notch (long and short). The moment carrying capacities, ductility, failure modes, moment - mid span deflection relations, bending moment capacities were presented. The results also show that the notched CFST specimens had lower mechanical performances than the intact CFST specimens. Furthermore, the investigating notch in the bottom more effect and danger to the structures when compared with the notch top and sidewall for (2 mm, 4 mm), in addition to the notch in the bottom had less than ductility from top and sidewall.

Keywords: Self compacted concrete (SCC), Concrete Filled Steel Tube (CFST) beams, notches, flexural strength, ductility.

`

ÖZET

DAİRESEL KESİTLİ İÇİ BETON DOLDURULMUŞ ÇELİK TÜP KİRİŞLERİN EĞİLME DAVRANIŞINDA KUSURLARIN ETKİSİ

ALHETE, Omar Ali
Yüksek Lisans Tezi, İnşaat Mühendisliği Bölümü
Danışman: Dr. Öğr. Üyesi Mehmet Tolga GÖĞÜŞ
Eylül 2018
54 sayfa

Çelik tüplerin malzeme kusurlarının kiriş eğilmesi üzerindeki etkilerini araştırmak için bu tezde, çelik borularda yapay çentikli İçi Beton Doldurulmuş Çelik Boru (İBDÇB) kirişlerin eğilme testleri yapılmıştır. Bu çalışmada, çelik borudaki çentikli İBDÇB kirişlerinin eğilme davranışları, 24 adet çentikli İBDÇB kirişleri, iki adet (kontrol) çentiksiz İBDÇB kirişleri olmak üzere 26 adet numuneden oluşan set iki farklı kalınlık (2mm, 4mm) olarak incelenmiştir. Kendiliğinden yerleşen beton (KYB) doldurulmuş çelik boruların eğilme performansını araştırmak için İBDÇB üstten, alttan ve yan yüzlerinden iki farklı kalınlıkta ve iki farklı çentik uzunluğunda (uzun ve kısa) sahip çentiklerle kirişler üretilmiştir. Moment taşıma kapasiteleri, süneklik, göçme modları, moment - orta açıklık deplasman ilişkileri, eğilme momenti kapasiteleri sunulmuştur. Sonuçlar ayrıca çentikli İBDÇB numunelerinin kontrol İBDÇB numunelerinden daha düşük mekanik performanslara sahip olduğunu göstermektedir. Ayrıca, çentik üst ve yan yüz (2 mm, 4 mm) ile karşılaştırıldığında, altta daha fazla etki yaptığı ve yapılara yönelik tehlike oluşturduğu incelenmiş, ek olarak alttaki çentiğin üst ve yan yüzlerden daha az sünekliğe sahip olduğu görülmüştür.

Anahtar Kelimeler: Kendiliğinden yerleşen beton, içi beton ile doldurulmuş çelik tüp kirişler, çentikler, eğilme dayanımı, süneklik.

To my parents….

`

ACKNOWLEDGEMENT

I would like to express my special appreciation and thanks to my supervisor Asst. Prof. Dr. Mehmet Tolga GÖĞÜŞ, for all his help, patience, valuable advice, always providing and guiding me in the right direction. I am very grateful and proudest to work under his academic guidance.

I would like to express truthful appreciation to Dr. Ahmed Abdulhafedh. Special thanks to my family. Words cannot express how grateful I am to my father's spirit that his words lead me to receive my mother's testimonies and sacrifices for all my sacrifices and for the great support I have received from my dear wife as well from the good words of my brothers and sisters and the help that I have received from my friends and thank them so much.

`

TABEL OF CONTENTS

`

LIST OF TABLES

Page

`

LIST OF FIGURES

Page

CHAPTER 1

INTRODUCTION

1.1 General

The composite members consisting of steel tubes filled with concrete construction structure provides numerous structural advantages contain high strength and fire resistance, high energy absorption capacity and favorable ductility. There is also no need to use a shutter during concrete construction. Therefore, time and construction costs are reduced. These advantages are widely used and have resulted in widespread use of concrete in-filled tube structures in civil engineering structures (Han et al., 2014). Also used all over the world is used as a primary lateral resistance from a compression member of an open-floor plan of a low-rise structure utilizing cold-formed steel tubes in-filled with in-situ concrete large caliber cast in situ or precast. (Ghannam, S. 2016). In modern buildings such as bridges, high-rise buildings, transmission towers, warehouses, etc., Concrete-Filled Steel Tube (CSFT) structures have become widespread in recent years. In the long term, it will compete against strength, high ductility, large energy absorption and high rigidity, The difficulty of compacting concrete is that concrete bleeding can create weaknesses in the system that creates gaps between steel and concrete.to recompense for this drawback, raised on concrete quality with low water content and super plasticizer agent for improving workability are used for construction (Morino and Tsuda, 2003). Because concrete filling arrangement does not require vibration, it can be further strengthened by using Self-Compacting Concrete (SCC) (Hanetal, 2006), Furthermore, since the steel tube surrounding the concrete can act as a permanent mold like other metal structural parts, imperfections always exist in the external steel tube of the CSFT member and the possibility of structural disadvantage there are significant impacts on honesty and lifespan that can reduce person-hours and effort. Imperfections of steel members can be generally categorized into two main types: geometric imperfections and material imperfections.

The former is the actual geometrical dimensions and is due to manufacturing tolerances, damage during the hand line process, or the effects of dent and permanent deformation of the steel member. Imperfections in materials are primarily related to defects or thickness variations due to corrosion welding or other chemical attacks. Geometric imperfections of cylindrical steel members have been intensively studied over the past decades, including shape and amplitude, impact on buckling strength, resulting design tolerances and design strength. Recently geometric imperfections on the compression behavior of cylindrical steel members for thin walled cylinders with material imperfections, buckling modes and strengths have been investigated.

In recent years, CFST members are used for deep ground clearance tunnels and mine road support systems. In such a case, it is necessary to notch pure concrete to the outer steel tube. On the other hand, steel tube outside the CFST members can cause corrosion and material defects when used in an aggressive environment. As mentioned above, the influence of material imperfections on steel cylinders has been extensively studied. However, little attention has been paid to the evaluation of defective CFST members. In these theses, we will investigate the behavior of steel tube s under loads, when they are subjected to notches shapes and bending to overload, although they have many advantages.

Numerous structures have reached the end of their useful life due to deterioration or deterioration due to environmental factors, or the need for increased application load or change in functional use. However, members of CFST need to strengthen, rehabilitate, and rehabilitate for various reasons Such as steel structures, may permanently contain defects as in the metal tubes that are outside of the CFST members, which may result in structural weaknesses and are ineffective, thereby reducing their lifetime in the buildings. The structural defects of the square or circular steel tubes in the past years, including their size, general shape and capacity, and the effect of the bending force and the differences resulting from the planning, design and the places of power in this form, have been thoroughly investigated and followed up for the purpose of study and find the appropriate way to treat them and assess the risk when they get.

1.2 Objective of Study:

The main objective of the thesis is to investigate the influence of material imperfections of outside steel tube on the mechanical performance of a circular concrete filled steel tube beams subjected to bending load. The artificial notches throughout the wall thickness of steel tube were used to represent the material imperfections. A series of specimens with notches in the steel tube was tested and the influences of various characteristics of notches, such as orientation, notch length and notch place on the failure modes, and load capacity of the circular concrete filled steel tube beams, were experimentally investigated. The load–displacement responses, beam strength and confining effects were discussed in detail.

1.3 Outline of the Thesis

Consists of five-chapter summary and abridgment of each chapter are given as below:

Chapter 1. Introduction:

The intention and scope of the thesis were presented.

Chapter 2. Literature review:

The main objective of the thesis is to investigate the influence of material imperfections of outside steel tube on the mechanical performance of a circular concrete filled steel tube beams subjected to bending load. The artificial notches throughout the wall thickness of steel tube were used to represent the material imperfections. A series of specimens with notches in the steel tube was tested and the influences of various characteristics of notches, such as orientation, notch length and notch place on the failure modes, and load capacity of the circular concrete filled steel tube beams, were experimentally investigated. The load–displacement responses, beam strength and confining effects were discussed in detail

Chapter 3. Experimental investigation:

This chapter provided an explanation and experimental investigation about the CFST beam with applying for notch in circular steel tubes.

Chapter 4. Results and discussion:

Results obtained from the notch in CFST and comber control beams of CFST beams with different size were given. Discussion on the results of the study was defined in this chapter.

Chapter 5. Conclusions:

Provide conclusions and summary based on the results of comparative investigations of this study.

Chapter 2

LITREATURE REVIEW

2.1 Concrete Filled Steel Tube Members

CFST members take advantage of both concrete and steel. These consist of a circular, rectangular, or square steel hollow section filled with normal or reinforced concrete. They are using widely as a beam of low-rise industrial buildings that require a rugged and efficient structural system and as high-rise buildings such as columns, beam-columns.

Lai (2014) presented the evaluation and development of these design provisions. The CFST members have been reviewed available experimental databases and a new experimental database of tests performed on non-compact and slender CFST members has been compiled. Detailed 3D Finite Element Method (FEM) models have been developed for non-compact and slender CFST members and benchmarked using experimental results. Design provisions of the American Institute of Steel Construction (AISC) 360-10 for non-compact and slender CFST members have been evaluated by experimental test results and additional FEM analysis dealing with experimental database gaps. The current AISC 360-10 axial load bending moment (P-M) interaction equation has been updated using the results of a comprehensive parametric study (directed using a benchmarked FEM model). Effective stress-strain curves of steel tubes and concrete filled have also been advanced. Validation of these effective stress-strain curves has been confirmed by implementing them in a macro model based on benchmarked nonlinear fiber analysis.

Alfawakhiri (1997) presented additional experimental data on the behavior of these structural elements and assess recent design code provisions with regard to circular CFST columns. Three long beam-columns (L/D = 13.5) have been tested under continuous axial compression and incrementally enhanced lateral displacement reversals. In addition, one short column was tested in concentric compression. All specimens had the same cross-sectional geometry to allow for direct comparison. Both strength and deformability issues were addressed. Various aspects of concrete confinement in circular CFST were analyzed. A comparative study of North American and European design code provisions was carried out. The result of the test indicates that by using of high strength concrete for circular CFST members does not cause any dramatic changes in the behavior. North American codes were shown to be more conservative than Euro code 4, but all codes gave conservative predictions of strength compared to the experimental results. A less conservative design approach was recommended for Canadian Standards Association (CAN/CSA-S16.1-94).

Elchalakani et al. (2001) showed investigational studies on the bending behavior of circular CFST subjected to large deformation pure bending of D/T 12 to 110 have been conducted. Their paper compares the behavior of void-filled and empty, circular hollow cross-sections cold-formed under purely plastic bending. The concrete filling has been found to completely prevent local buckling and elliptification of cold-formed steel tube with 13 < D/t < 40, but in the inelastic range of CFST of 74 < D/t < 110, A plastic ripple has been detected. Energy absorption, strengthening, and ductility is thinner than in the case of, particularly thick CHS. The plasticity limit of D/t 112 has been obtained for a CFST constructed under a pure bend from a cold-formed hollow section.

Chitawadagi et al. (2009) prepared a paper on the strength deformation behavior of circular steel tubes in-filled with concrete of different grade under bending. The influence of steel tube thickness, concrete filling strength, concrete cross sectional area and concrete confinement on moment capacity and curvature (CFST)s were investigated. The measured flexural strength is compared with the value predicted by EC 4-1994, Load, and Resistance Coefficient Design (LRFD) - AISC - 1999 code specification. A total of 99 specimens with all lengths of 1 meter was tested with concrete filling with characteristic strengths of 20, 30 and 40 Nmm2 and a (D/t) ratio of 22.3 to 50.8.

Based on the investigational results, an interaction model has been developed to foresee the moment and curvature of the CFST specimens. The results indicate that in the experimental investigation are used to all the hollow section resistance moments and the corresponding increase in curvature showed higher ductility than the hollow. The ductility and moment of resistance of both the hollow and the CFST sample are increased by increasing the wall thickness of the steel tube. For a given wall thickness of the CFST specimen, increasing the strength of the filled concrete will not help to significantly increase its capacity. The Strength Increase Factor (SIF) proposed here helps to estimate the concrete contribution to the moment capacitance of the CFST beams. Detention of infill contributes of concrete to higher performance while higher strength infill concrete has been utilized for higher wall thickness steel tube. Furthermore, EC 4-1994 foresees the moment capacity of the test specimens moderately in the range of 30% to 35%. Since the influence of concrete filling is not taken into consideration and AISC / LRFD is also the same, it is very conservative to predict the moment capacity of the CFST section.

Han et al. (2014) studied the development of the family of (CFST) structure until now, and draw out the research framework of CFST members. Figure 2.1 shows a cross-section of a typical CFST. Recent CFST structural members, especially research and development in China, have been summarized and discussed. Several projects in China utilizing CFST members have also been introduced. Finally, some conclusions are given for CFST members.

The results observed that the rapid development of research and application of CFST structures in China and all over the world in the previous decades, the scope of "CFST" is extended greatly by researchers and engineers. The characteristic of these CFST members is that the structural properties can be improved due to the "composite action" between filled concrete and steel tube. Basic design approaches from various countries and some typical applications of CFST members in buildings, bridges, and other structures are presented and compared. The CFST structure can be treated as a substitute system to the steel or the concrete reinforcement.

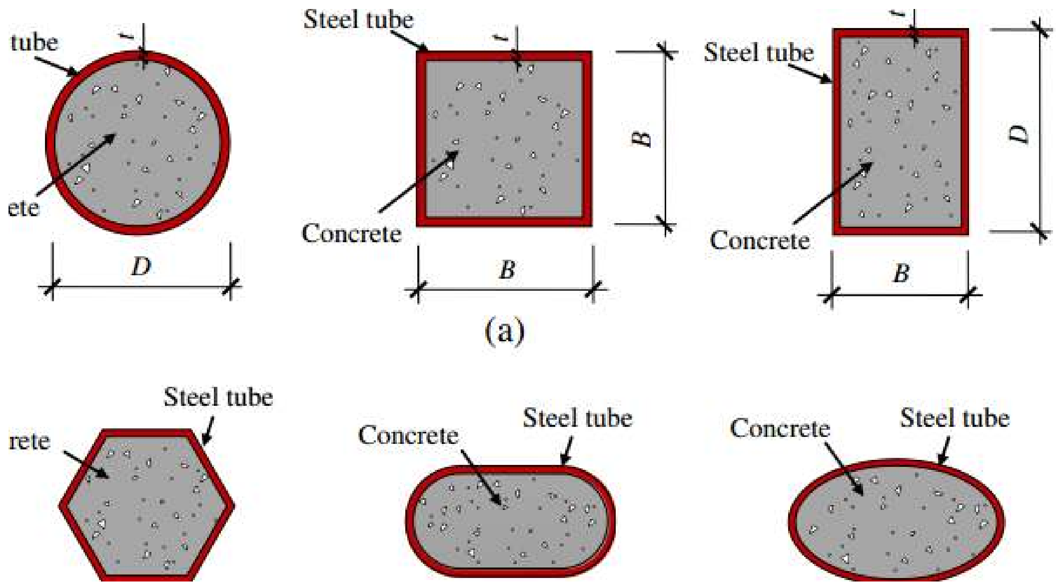

Figure 2.1 Typical concrete-filled steel tubular cross sections.

Ghannam (2016) studied an experimental investigation of the bending behavior of a square (CFST) subjected to pure bending, as shown in Figure 2.2 where the depth to thickness ratio (D/t) is 23.8 and 27.8. In this paper compares the behavior of rectangular hollow hot rolled sections concrete infill and empty under pure bending. The behavior of CFST beams partially replaced with coarse aggregate using granite under bending load has been shown. The effect of steel tube, concrete compressive strength and concrete confinement were investigated. Six specimens were tested at the concrete strength of 20 Mpas. The beam has been 88.9 × 88.9mm, 114.3 × 114.3mm, and the length has been 1200mm.

From the result of tests, it has been found that the ultimate load carrying capacity of the steel tube beam in which the coarse aggregate is partially replaced with granite is nearly the same as the concrete conservative. Generally, filled steel tubes increase ductility, strength and energy absorption, especially for the thinner section. The steel shell results in restraint of the concrete core, resulting in improved ductility and strength of the core.

Tao, Z., & Han, L. H. (2006) described a chain's of tests performed on Concrete In Filled Double-Skin Steel Tube (CFDST) stub columns, beams, and beam columns. Rectangular Hollow Section (RHS) cold-formed both outside of the tube and inside of the tube. The fracture mode and load deformation behavior of CFDST specimens have been compared with those of conservative CFST members and empty double-skin tube members. The results observed that the CFDST members showed behaviors similar to the conservative CFST specimens in the current test. Improvement in strength and ductility were observed for CFDST (RHS inner and outer) stub columns, beams and beam columns due to the composite action between the concrete core and the steel tube. A theoretical model has been advanced to foresee the load versus deformation relationship of CFDST stub column, beam and beam column. A good agreement has been attained between the prediction curve and the experimental curve. Simplified models were advanced to assess the strength of CFDST beam-columns, beams and columns. With reasonable agreement achieved, all predictions were compared with the result of tests.

Li et al. (2015) presented both experimental and numerical investigations on CFST tension members subjected to eccentric loads. Experimental parameters include load eccentricity and cross section steel ratio. Failure modes showed that in-filled concrete workings efficiently on steel tube and outside of tube improves concrete

Crack pattern and FA modeling was used to predict the same result. The failure mode of CFST tension member subjected to eccentric load is a combination of elongation and all-inclusive bending. Composite members subjected to all eccentric loads showed large deformability when the rotation of the end exceeded 0.1 rad. The compressive area may happen in the composite section while the member receives an eccentric load. Due to the composite effect of steel and concrete, the strength of composite specimen was much greater than hollow steel tube. The linear tension-to-moment interaction relationship shows acceptable results for CFST members. The recent design equation gives a safe and conventional estimate of the tension and flexural strength of CFST tension members subjected to eccentric loads.

Zhou et al. (2017) studied the mechanical behavior of the circular (CFST) s under axial tension. A group of three circular CFSTs with different steel ratios and in-filled concrete diameters are tested and compared with Hollow Steel Tubes (HTs). Based on the experimental results in the present and previous studies, three key issues of circular CFSTs under tension, i.e. the confining-strengthening effect, the confining stiffening effect, and the tension-stiffening effect, are studied at both the stress-resultant level (i.e., force displacement relationship) and stress levels (i.e., stress-strain relationship). At the stress-resultant level, the test results demonstrate that the strength and circular stiffness CFSTs are average 10% and 29% larger than those of HTs are, respectively. The strength increase is contributed by the confining-strengthening effect, and the stiffness improvement is a combined result of the confining stiffening and tension-stiffening effects. At the stress-strain level, the measured strains show that the steel tube of the circular CFST is in the state of the bi-axial tensile stress state because of the difference of the Poisson's ratio between steel tube and in filled concrete, which contributes to the confining strengthening and confining-stiffening effects of the circular CFST.

Roeder et al. (2010) studied the combination of axial force and bending load and decided the best model to predict stiffness and circular resistance CFST. 122 specimen databases have been gathered and assessed.

The result shows that the plastic stress way is a simple but effective method to predict the resistance of a circular CFST component under combined load. These data indicate that the current specification provides an inexact prediction of flexural stiffness and a representation of new stiffness is suggested. The suggested model allows simple but exact prediction of resistance and stiffness, allowing engineers to routinely use CFST constituents in structural design.

Varma et al. (2002) investigated the experimental behavior of square CFST columns witches made from high strength material. The influence of steel tube width to thickness ratio, yield stress and axial load level on stiffness, strength, and ductility of high strength CFST beam column have been studied. 16 3/4 scale CFST specimens containing 8 monotonic beam-column specimens and 8 cyclic beam-column specimens have been tested. Experimental results indicate that cyclic loading has no important influence on the strength or stiffness of the CFST beam column. However, it causes a more rapid diminution in the peak of post moment resistance.

Ammari et al. (2013) investigated the experimental behavior using the new system of the U-link of the CFST beam joining the concrete core on the compression side of the beam to the steel tube, resulting in a large confinement of the concrete core. Detention is attained by using the expected split-up between the two materials. As shown in Figure 2.3, two built-up CFSTs were experimentally tested to study the effect as reinforcement when U-link was used for a beam subjected to bending load. The state of the concrete in the tube did not show crash of the concrete when those beams have been cut at the position of the plastic hinge. Measurement of strain shown that the compressive strain of concrete is 5 to 6 times the crash strain of concrete. Investigational data exhibited that the use of a U-link as an added reinforcement in concrete filling tube improves beam bending capacity, stiffness, and ductility.

Vijay and Manoj (2014) presented a study on the flexural behavior of CFST based on the previous effort carried out by Manojkumar as shown in Figure 2.4. An ANSYS model has been developed that can predict the behavior of CFST to determine the moment carrying capacity at ultimate point. The CFST beam is verified and verified against experimental data by the finite element method program ANSYS. The main parameters affecting the behavior and strength of concrete filled beams, geometric parameters, material nonlinearity, load, boundary conditions, and the degree of concrete containment. To account for all these characteristics, the ANSYS model has been developed. The main parameter that changes in analytical research is the D/t ratio, which is the characteristic strength of filled concrete. The suggested model foresees the ultimate moment capacity of the CFST beam. For numerical analysis, circular and rectangular CFST cross sections are taken into account using different grades of concrete. Compare the predicted value with the experiment result. Numerical analysis shows that a good confinement effect can be obtained with a rectangular CFST.

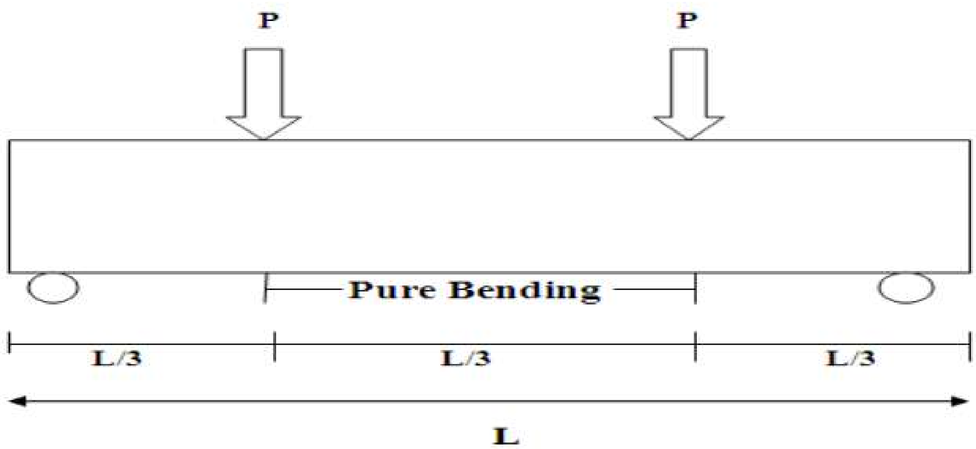

Figure 2.2 Flexure test on CFT beam (Vijay and Manoj, 2014).

Han (2004) developed a mechanics model that can expect the behavior of concrete infill Hollow Structural Section (HSS) beams. A series of rectangular and square CFST beam tests were performed. The main parameters varied in the tests were the depth to width (H/B) ratio and tube depth to wall thickness ratio. The relationship between load and lateral deflection was recognized for CFST beams both theoretically and experimentally. The results observed that the CFST beam behaved relatively ductile and the test continued in a smooth and controlled manner. The moment capacity of HSS beams could be conservatively predicted by using the recommendations of Architectural Institute of Japan (AIJ 1997), British Standard (BS5400 1979), EC4 (1994), LRFD-AISC (1999), and the suggested model in their paper. Generally, AIJ (1997) and LRFD-AISC (1999) showed moment capacity about 20% lower than the test. In addition, BS 5400 (1979) showed a moment capacity about 12% lower than the test. Also, the method suggested as EC 4 (1994) predicted a capacity about 10% lower than the result of the test.

Han et al. (2006) studied the flexural behavior of 36 composite beam specimens infill with Self-Concrete Concrete (SCC). The main parameters that change in the test are as follows. (1) The ratio of tube diameter-to-wall thickness. (2) Steel yield strength; (3) Section type. A comparison is made with the beam capacity predicted using the existing method. In general, the CFST beam filled with SCC was found to be very similar to the beam of composite beams filled with normal concrete. Simplified models for computing the moment versus deformation relationship of the composite beam have been advanced. Moment versus curvature relationships between mechanic models, test results, and simplified models are compared and generally, good agreement is achieved.

Lai (2015) presented the basis of the current AISC specification (AISC 360-10) on the design of non-compact and circular of slender CFST members under axial compression, bending, and combined-load. An investigational test database performed on compact, circular of slender CFST members have been collected and used to create maintainability of AISC specification design equations. Comparison with both the experimental results and finite element analysis showed that the circulating force of CFST members can be calculated conservatively using the (AISC 360-10) design equation.

Oyawa et al. (2004) sought alternative filling materials (polymer base) for very limited cement concrete used in CFST construction. Polymers are successfully used in other industries, are lighter, tensile strength is high, are durable and are known to withstand destructive environments. The results of this study on the least-plastic properties of homogeneously bending polymer CFST beams show an enormous increase in composite beam stiffness, strength, and ductility in empty steel tubes.

Results revealed that it became clear that epoxy polymer concrete creates composite steel beam with greatly improved strength and ductility. Epoxy polymer concrete has a wide range of interactions with steel sections because of low tensile, compressive, and low inward motion of the cross section neutral axis due to high tensile adhesion even in the inelastic range.

Keara's et al. (2013) presented a method for designing a hollow and solid CFST beam based on test data. This is because the limit of increasing the strength of concrete due to detention contravenes the recommendation of 6.7.2 and full composite action of concrete and steel is assumed because conformity with the test result is better than EC 4 (CEN 1994). The proposed analytical method shows a good agreement with the natural and numerical test results with a hollow and solid CFST beam and makes it possible to recommend the method presented in such an efficient composite beam design practice.

Mohiuddin et al. (2016) investigated the flexural properties of CFST partially replaced with coarse aggregate. Their paper showed the use of CFST beam partially replaced with coarse aggregate by 10% and 30% under loading and an attempt has been made using recycled aggregate instead of convention aggregate Results concluded that the use of recycled aggregate up to 30% in CFST have similar strength while compared with that of normal plain reinforced beam. The ultimate load of steel tubular beam infill with normal concrete is about 42.30% increase than that of the hollow tubular reference beam and the percentage decrease of partially replaced coarse aggregate with infill normal concrete is about 2.73%, 4.37%.

Arivalagan et al. (2010) presented a study on the flexural and cyclic behavior of hollow beam sections of concrete infill steel. Test specimens in-filled with normal mixed concrete, fly ash concrete, quarry waste concrete and low strength concrete (brick - butt - lime concrete) and hollow steel sections have been tested. The beam capacity has been compared with the ultimate capacity achieved by international standards EC

4 - 1994, ACI - 2002 and AISC - LRFD - 1999. The investigational study revealed that the beam specimens compared to the hollow steel section increased the moment carrying capacity of ordinary mixed concrete 28%, fly ash concrete 27% and quarry waste concrete 25%. Concrete filled increases the residual-load capacity of thin SHS and RHS beams that withstand cyclic loads, especially while increasing lateral displacement and also increasing the energy absorption of hollow steel sections.

Soundararajan and Shanmugasundaram (2008) have experimentally studied the contribution of the normal mix, fly ash, quarry waste and low strength concrete (brickbat lime concrete) to the ultimate moment capacity of the hollow square steel. The same dimensions of 15 simple supported beam specimens of 1200mm long steel hollow sections in-filled with normal mixtures, quarry waste, fly ash and low strength concrete and identical dimensions of hollow sections have experimented. These experimental findings showed that normal mixes, fly ash, quarry waste and low strength concrete enhance the moment carrying capacity of steel hollow sections. Mohanraj et al. (2010) showed experimentally investigation of the bending behavior of square CFST while D/t ratios were 23.6 and 25.4. Their papers compare the empty and void filling behavior of hot rolled square hollow sections under purely plastic bending. Partially replaced with fine aggregates by using fly ash and quarrying dust and by partially replaced with coarse aggregate and granite, construction and demolition debris, rubber, steel slag, tiles and marble behavior of square CFST beams have been presented. The steel tube effects, concrete compressive strength, and concrete detention have been investigated. In their study, 20 specimens were tested at the concrete strength of 20 Mpas. The beams have been (91.5 x 91.5) mm, (113.5 x 113.5) mm cross section and 1200 mm long. From the test results, it has been detected that the ultimate loading capacity of steel tube beams infill’s with different waste materials, concrete is about the same as conservative concrete. Generally, void filling of steel tubes improves ductility, energy absorption, and strength, particularly of thin-walled sections.

2.2 Effect of notches in beams:

They are slots that infect the iron or concrete structures because overloads or presence in aggressive environment causing various structural damage, the notches in beams reduce the effective area available to resist shear and bending moment and should be taken seriously. In the case of large openings, it is necessary to replace the lost area by adding plates or stiffeners approximately the hole or the notch. Any removal of material will certainly weaken the structure in some cases; the effect of penetration may be small, either due to its location or due to its size. In other cases, however, the decrease in strength can be significant and local strengthening will be required.to calculate whether a particular penetration is significant in terms of the strength of the beam, two relevant factors must be looked at. These are:

- The location of the penetration
- The size of the penetration.

To understand the effects of notches one must consider five parameters: Concentrations of stress and of strain stress gradients. mean stress effects and residual stresses. local yielding development and growth of cracks. To locate the holes or notches we need to examine both, the cross section and the span location.

If we choose a spot on the section where bending stress is minimal at the neutral axis, it happens to be the area where shear stress is maximum. Likewise, along the span, bending stresses are generally low near the supports but shear stresses are the highest over there. The artificial notches through-out the wall thickness of steel tube were used to represent the material imperfections from corrosion or other damages. Series of specimens with notches in the steel tube was tested and the influences of various characteristics of notches, such as orientation, notch length on the failure modes, and load capacity of the CFT beams, were systematically investigated. Notches to the flanges or webs of beams or to studs or slabs can be significantly detrimental to the structural integrity of an element experiments and tests were completed to ascertain the extent of the engineering errors and defects in the performance of the square tubes. Stull, J.M. Nichols, (2011) he also was studied the extent to which engineering defect or engineering defect in the structure of the crust. Alavi Nia, H. Badnava, K.H. Fallah Nejad, (2011) He also investigated the impact of falling collapse on the properties of the tube response to the energy absorbed by the square-shaped tubes if under the influence of the semi-static force in a tilted manner. Sadovsky, J. Krivacek, (2012), describe the computational modeling of engineering defects and the hardness of cold-formed steels. Zhang, (2009) studied the energy absorption of the square powder tube axially with the twisting starter. For thin-walled steel tube panels with physical defects, their torsion and strength patterns have also been verified in recent years. Alavi Nia et al. (2011)the effect of cracks on the properties of energy absorption of square tubes and tubes with cylindrical shape where they made these cracks in different positions as well as the nook of those cracks were different. Han (2012) studied parts of rectangular steel tubes by lifting a load to measure the erosion and impact of loading in that part. Estekanchi, A. Vafai, (1999) also studied by experimenting with the sureness of the twisting process that gets in the plastic cylinders containing the reinforcement. Julien, A. Limam, (2004) also conducted an investigation into the effect of sizes, shapes, cracks and location on the compressive load strength of these cylinders. Contributions from missing locations, related to border conditions, properties of materials, and crust with thickness, were also important for consideration. As an attempt to investigate the effect of local structural defects on the steel tube on the mechanical performance of CFT packages, Tao, Liao, (2006) function related to local imbalance was used as a numerical example. Between the test result and the FE result, the behavior of the torsion, in the conversion response of the load and the final force are equally large. Zhang, (2009) studied the design defects of steel tubing related to the mechanical behavior of CFT packages.

2.3 Artificial notches:

The artificial notches through-out the wall thickness of steel tube were used to represent the material imperfections from corrosion or other damages. A series of specimens with notches in the steel tube was tested and the influences of various characteristics of notches, such as orientation, notch length on the failure modes, and load capacity of the CFT beams, were systematically investigated.

CHAPTER 3

EXPERIMENTAL INVESTIGATION

3.1 General

The experimental investigation was accepted to study the structural performance of CFST beams with applying the effect of notch in CFST beam. The study focused on the flexural bending behavior through a series of twenty-four CFST and two control steel tube beams. The parameters considered are the effect of applying notch in CFST on the flexural behavior as compared to control beams. The specimens are examined to measure the behavior in term of the moment-deflection, moment carrying capacity and their strengthened behaviors. This chapter presents details and properties of the materials are used to construct the specimens and testing of the specimens.

3.2 Material Properties

3.2.1 Self - compacted concrete

In this study, the mix proportion of the SCC consisted of Water (W), Super Plasticizer (SP), Cement (C), Fly Ash (FA), Natural Fine Aggregate (NFA) with 4mm maximum particle sizes, Crushed Sand (CS) with range of particle sizes are 2-0.3mm, and <0.3mm as finer, and Natural Course Aggregate (NCA) with 10mm maximum particle sizes are used. The mix design is done for C40 grade, the water cement ratio is used as 0.33 and the mixing ratio of the SCC the Table 3.1 below. The mean compressive strength of the mix proportion is determined in the laboratory at testing day after casting of three cylinders 100mm by 200mm as shown in figure 1. The average concrete compressive strength is 49.33 MPa, shown Figure 3.1.

Table 3.1 Mix proportions for C40 SCC.

Mix proportions	W/B	C	FA	W	SP	CA	NS	CS (20. 3mm)	CS (0.3mm)
Kg/m^3	2338.3	285	285	188.1	2.7	709.8	651	144.6	7.23

Figure 3.1 Mixing of the SCC

(A) (B)

Figure 3.2 (A) Concrete cylinders before testing, (B) Concrete cylinders after testing.

3.2.2 Steel tubes

This study consists of 26 beam samples. All steel tubes are manufactured from two cold hollow circular sections with a length of 6 meters. The nominal dimensions of the rectangular steel tube sections were 820 x 100 x 2 mm, 820 x 100 x 4 mm. The width to depth of notch ratio (D / T) of the samples ranges. Three coupons of each tube were cut from three sides of hollow steel sections to find the properties of the actual material. Tensile coupons were taken from all faces except for the welded face in the tubing to avoid uneven power due to welding. The tensile strength tests were performed and tested in accordance with the recommendations of ASTM E8 / E8M-15a (2015) (ASTM E8 / E8M-15a, 2015) shown Figure 3.3.

Figure 3.3 Tensile after testing

3.2.3 Specimen properties

Two types of tubes s were cut and formed with a thickness of 2 mm and 4 mm long, circular steel in shape with a length of six meters and formed to the required length, ensuring that there are no irregularities in the shape. The interior faces of the beam samples have been cleaned to remove any rust or debris, and the grease and oil deposits, if any, are cleaned. 26 radial samples were prepared from circular sections of length 82 cm for testing in this study. The 26 samples consist of notches of different dimensions and places of existence in the model where the length (5 cm and 2.5 cm) and the direction (vertical and horizontal) are once in (top and bottom and once in the side) respectively (5 times horizontal and 5 times vertical and once 2.5 horizontal and 2.5 vertical times in each of the top, bottom and side) and for both thickeners, two CFST packages without any reinforcement (control beams). The samples were divided into six groups according to the location of notches in the steel tubes. Each set contains four samples plus a control sample to compare with each time. The dimensions and details of each sample are listed in Table 3.2.and Figure 3.4 illustrate with full details.

The following labeling system was used to assign each sample of the packages in Table 3.2. Where, C100-4, C100-2, Nos. 4 and 2 refer to the thickness of the tubes and the c character indicates that it is circular and the number 100 indicates the diameter of the tube, The character (B) represents the width. The character (H) represents the depth for the notch. The letters T, S and B represent the notch of the form in the form (top, side and bottom) and the letter V indicates that the vertical and character H is not horizontal and the letter L is notch 5 cm and that the letter S is notch length 2.5 cm For example, one set of beam samples, C100-4-TLV, is a 4mm circular beam sample with a notch length of 5 cm at the top and a vertical direction. Another example of the model named C100-2-BSH means that this model is circular with a diameter of 100 mm and thickness of 2 mm contains notch short at the bottom and horizontal direction and so on for the rest of the models.

The removable silicon later to prevent the leakage of the concrete mixture from which the steel tubes are held upright in the concrete-prepared rack closes the notches. The bottom ends of the steel tube are tightly covered with 3mm steel thickness by welding. Of each set, the other control package in the filled SCC without notch as shown in Figure 3.4 then SCC bars in the steel tubing of the top without any pressure. After the filling, the concrete is cut using a shovel as shown in Figure **5**. After the treatment period, in the event of any shrinkage, the gap is sealed using epoxy and then covered with other steel plates by welding; a metal angle is installed on the model for carrying the LVDT shown Figure 6, Samples were prepared for testing**.**

Figure 3.4 Specimens before casting

(A) Specimens after casting

(B) Specimens after casting

(**c**) Specimens curing

Figure 3.5 A, B and C specimens after casting and curing.

Table 3.2 Design beams and notches 4mm top.

Group name	Designation of beams	orientation	location	$l \times b$ (mm)	D × t × H* (mm)
GR 1	Control-4mm				100×4×820
	C100-4-TLH	horizontal	top	50×4	
	C100-4-TLV	vertical	top	50×4	
	C100-4-TSH	horizontal	top	25×4	
	C100-4-TSV	vertical	top	25×4	

* 100×4×820 dimension for all specimens is equal

Table 3.3 Design beams and notches 4mm bottom.

Group name	Designation of beams	orientation	location	l × b (mm)	D × t × H* (mm)
GR 2	C100-4-BLH	horizontal	bottom	50×4	100×4×820
	C100-4-BLV	vertical	bottom	50×4	
	C100-4-BSH	horizontal	bottom	25×4	
	C100-4-BSV	vertical	bottom	25×4	

*100×4×820 dimension for all specimens is equal

Table 3.4 Design beams and notches 4mm side.

Group name	Designation of beams	orientation	location	$l \times b$ (mm)	$D \times t \times H^*$ (mm)
GR 3	C100-4-SLH	horizontal	side	50×4	100×4×820
	C100-4-SLV	vertical	side	50×4	
	C100-4-SSH	horizontal	side	25×4	
	C100-4-SSV	vertical	side	25×4	

* 100×4×820 dimension for all specimens is equal

Table 3.5 Design beams and notches 2mm top.

Group name	Designation of beams	orientation	location	$l \times b$ (mm)	$D \times t \times H^*$ (mm)
GR 4	Control-2mm				100×2×820
	C100-2-TLH	horizontal	top	50×2	
	C100-2-TLV	vertical	top	50×2	
	C100-2-TSH	horizontal	top	25×2	
	C100-2-TSV	vertical	top	25×2	

* 100×2×820 dimension for all specimens is equal

Table 3.6 Design beams and notches 2mm bottom.

Group name	Designation of beams	orientation	location	$l \times b$ (mm)	$D \times t \times H^*$ (mm)
GR 5	C100-2-BLH	horizontal	bottom	50×2	100×2×820
	C100-2-BLV	vertical	bottom	50×2	
	C100-2-BSH	horizontal	bottom	25×2	
	C100-2-BSV	vertical	bottom	25×2	

* 100×2×820 dimension for all specimens is equal

Table 3.7 Design beams and notches 2mm side.

Group name	Designation of beams	orientation	location	$l \times b$ (mm)	$D \times t \times H^*$ (mm)
GR 6	C100-2-SLH	horizontal	side	50×2	100×2×820
	C100-2-SLV	vertical	side	50×2	
	C100-2-SSH	horizontal	side	25×2	
	C100-2-SSV	vertical	side	25×2	

* 100×2×820 dimension for all specimens is equal

3.2.3 Test procedure

The testing of beams is done by using of flexure machine test with 500 KN capacity. All beams are tested under simply supported end conditions and under two-point loading with displacement control loading method with a rate of 1mm / min. Since the support is fixed at a distance of 820 mm from both ends of the beam, the clear span is 750 mm. Two points loading is adopted for the test and it provides a net bending area of 250 mm. The axis of the sample is carefully aligned with the axis of the loading device. Three linear variable differential transistors LVDT are fixed along the length of the beam and measure the deflection. Of the three LVDT, two are located at a distance of 175 mm on both sides from the mid span, and the third mid span is precisely fixed in the mid span. All beams are loaded up to failure.

(A) Before load

(B) After load

Figure 3.6 A and B flexure test on effect of the notch in CFST beam before and after load.

CHAPTER 4

RESULTS AND DISCUSSIONS

After the age of testing day, all beams are prepared for testing. The beams have been loaded with equal force on the two load points until it did not take any further load. First, the effect of notch in beams has been compared with control tubes for all groups, it found that the concrete inside the tubes has significantly for increasing the beams moment carrying capacity and reduce the deflection; it means that the CFST have a stiffer response for loading until failure occurred. Second, notch, its dimensions and its location were observed in the beams in terms of the speed of failure of the model and its comparison with the control.

3.3 Failure Modes

The testing process continued smoothly and rigorously, and all tested specimens behaved and failed in a lengthy manner. The failure patterns are shown for all beam samples tested in Figs. 4.1 and 4.2. tube failure cases in all groups can be identified as follows either through the local torsion below the two loading points at the top edge if the notch is from the top and the horizontal direction, or torn if notch in the side and in the vertical direction, regardless for the width to depth ratio (D / T). On the other hand, the samples containing the notch failed at the bottom by rupture in the tube because of the load on the other hand. There are models where nothing happened during the examination. There was a total twist of the model without rupture. In the presence of the notch at the top or in the side or at the bottom and sometimes in the opposite side of the presence of notch. After dividing the specimens into six groups, The first group (TLV, TLH, TSV and TSH) was first class and the failure was on two types in the horizontal direction (5 cm and 2.5 cm) in which the local buckling occurred with the failure of the inner concrete. Either in the vertical direction has a blockage of the notch with the failure of the internal concrete shown Figure (4.3). The second group (BLV, BLH, BSV and BSH);

There was a rupture of the model at the notch end. Either vertical or horizontal according to notch direction shown Figure (4.4). The third group (SLV, SLH, SSV and SSH) were in the side as well as in two directions, one horizontal and the other vertical as in the other models. Notch on the long and short vertical direction begins to rupture from end notch tip, while the horizontal notch has only slight deformation in notch format shape dimensions shown Figure 4.5

The fourth group (TLV, TLH, TSV and TSH) was notch at the top where the local buckling of the notch was horizontal, while the distortion in vertical notch was the closure due to the effect of load on the model of the laboratory test shown Figure (4.6). The fifth group (BLV, BLH, BSV and BSH) was for tubes with a thickness of 2 mm and was notch from the bottom where the shape of the failure was rupture. Especially at the notch endings, where samples failed more quickly than samples with similar thickness of 4mm shown Figure 4.7

The sixth group (SLV, SLH, SSV and SSH) was notch in the side showing that the shape of the failure in the vertical direction is rupture, either in the horizontal direction there was no significant effect of the convex load where there was a slight deformation in notch dimensions shown Figure 4.8

(**A**) Sample no one C100-4-BSH of the first group failure modes

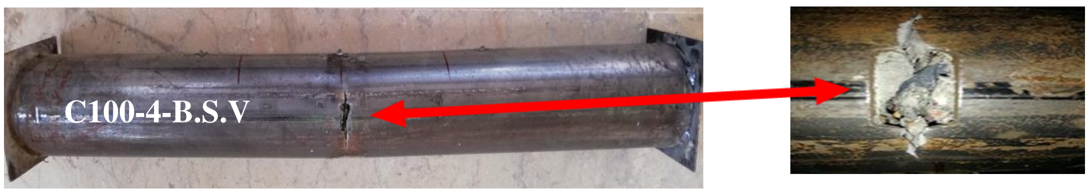

(**B**) Sample no two C100-4-BSV of the first group failure modes

(**C**) Sample no three C100-4-BLH of the first group failure modes

(D) Sample no four C100-4-BLV of the first group failure modes

Figure 04.1 A B C and D Samples of the first group failure modes

Figure 4.2 Samples of the first and second group after test

(**A**) Sample no one C100-4-TSH of the second group failure modes

(**B**) Sample no two C100-4-TSV of the second group failure modes

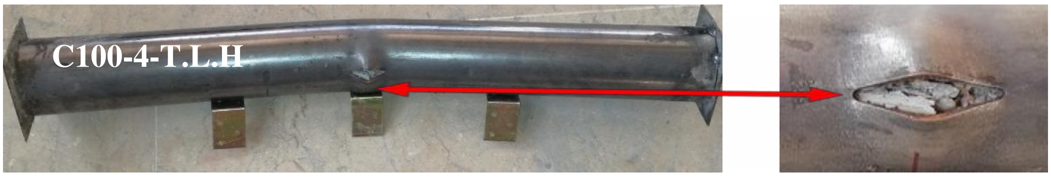

(**C**) Sample no three C100-4-TLH of the second group failure modes

(D)Sample no three C100-4-TLV of the second group failure modes

Figure 4.3 A B C and D Samples of the second group failure modes

(**A**) Sample no one C100-4-SSH of the third group failure modes

(**B**) Sample no two C100-4-SSV of the third group failure modes

(**C**) Sample no three C100-4-SLH of the third group failure modes

(**D**) Sample no four C100-4-SLV of the third group failure modes

Figure 4.4 A, B, C and D Samples of the third group failure modes

Figure 4.5 Samples third group after test

(A) Sample no one C100-2-BSH of the fourth group failure modes

(B) Sample no two C100-2-BSV of the fourth group failure modes

(C) Sample no three C100-2-BSH of the fourth group failure modes after the test

(D) Sample no four C100-2-BLV of the fourth group failure modes

Figure 4.6 A B C and D Samples of the fourth group failure modes

Figure 4.7 Samples of the fourth group after test

(A) Sample no one C100-2-TSH of the fifth group failure modes

(B) Sample no two C100-2-TSV of the fifth group failure modes

(C) Sample no three C100-2-TLH of the fifth group failure modes

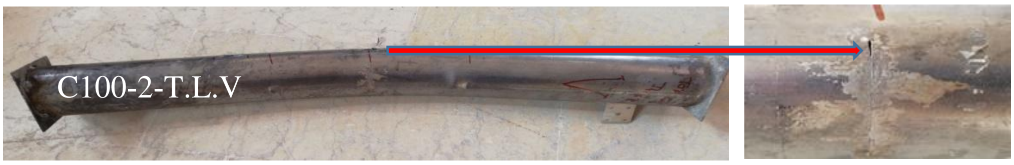

(D) Sample no four C100-2-TLV of the fifth group failure modes

Figure 4.8 A, B, C and D Samples of the fifth group failure modes

Figure 4.9 Samples of the fifth group after test

(A) Sample no two C100-2-SSV of the sixth group failure modes

(B) Sample no two C100-2-SSV of the sixth group failure modes

(C) Sample no three C100-2-SLH of the sixth group failure modes

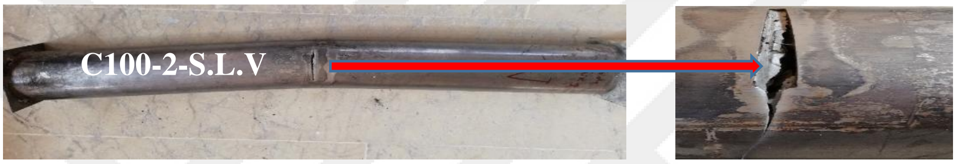

(D) Sample no four C100-2-SLV of the sixth group failure modes

Figure 4.10 A, B, C and D Samples of the sixth group failure modes

3.4 Moment mid span deflection curves

Figure (4.1. to 4.9) (a, b, c, d,) show the force displacement curves in beams for groups 1, 2,3,4,5 and 6, respectively. All beam curve curves showed smooth moments with large deviation until failure. The control beams were compared with steel tubes for all groups containing notch, where it was found that the concrete inside the tube significantly increased the capacity and rigidity of the tube. The test also showed that the extent of the notch impact on the behavior of the circular tube filled with concrete. Moment - mid span deflection relations. All models passed through three stages of linearity and then yielding and then failure. The first group (TLV, TLH, TSV and TSH) in the first group, the behavior of the models was close to the control where the notch was from the top and in two directions (horizontal and vertical) and length (2.5 cm and 5 cm). As in the rest of the models.

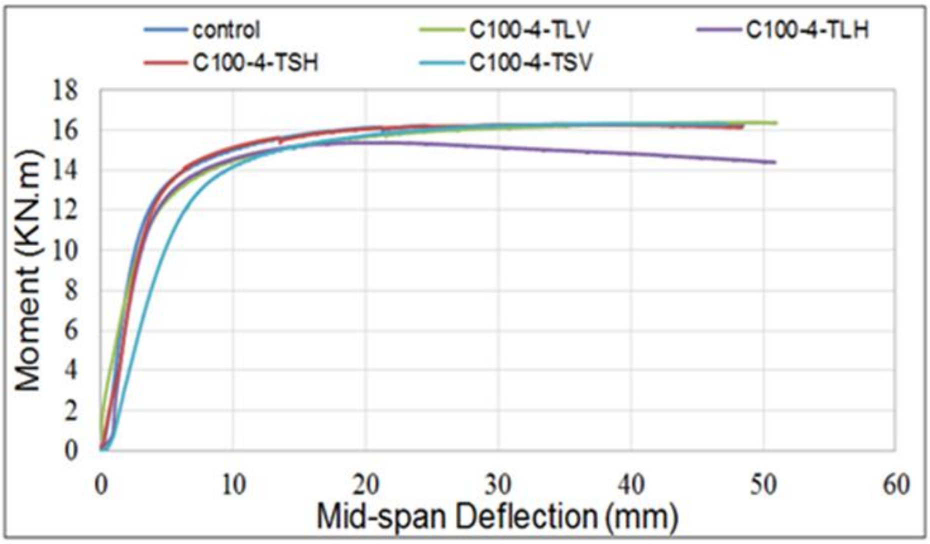

Figure 4.11 Moment capacity and mid span deflection for group one.

The second group (BLV, BLH, BSV and BSH) in this group were notch bottom. Some models were different from control. The vertical notch was more pronounced than the horizontal notch. The vertical notch failed at a time less than the control. On the horizontal notch, it took more time to reach the failure stage and were close to control.

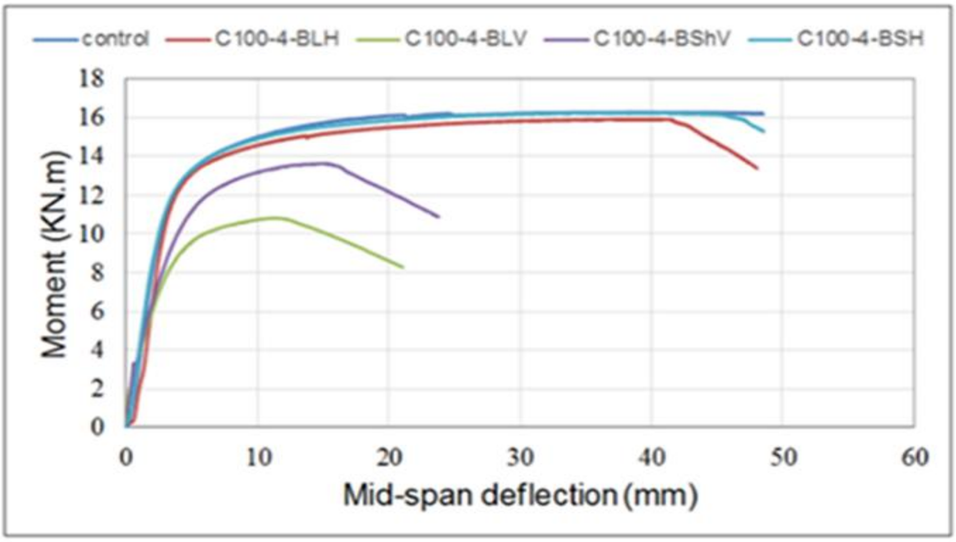

Figure 4.12 Moment capacity and mid span deflection for group two.

The third group (SLV, SLH, SSV and SSH) This set was notch in the side where the horizontal direction of the notch showed behavior soon to control either the notch had a different behavior where it failed more quickly compared with the control.

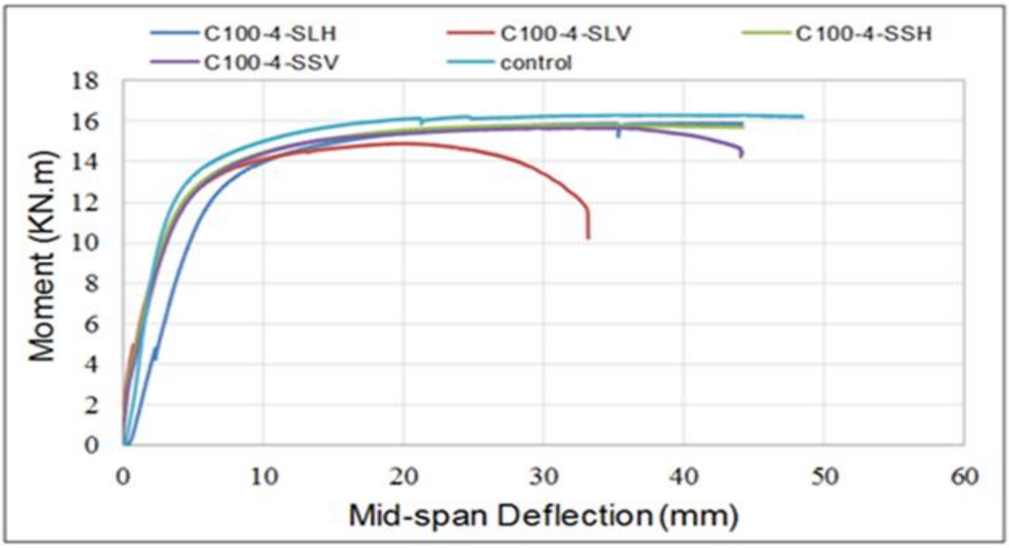

Figure 4.13 Moment capacity and mid span deflection for group three.

The fourth group (TLV, TLH, TSV and TSH) in this group the notch in top, three samples had similar behavior to the control, but only one model containing notch horizontal length of 5 cm had a different behavior where it reached the failure phase at a faster time than the control.

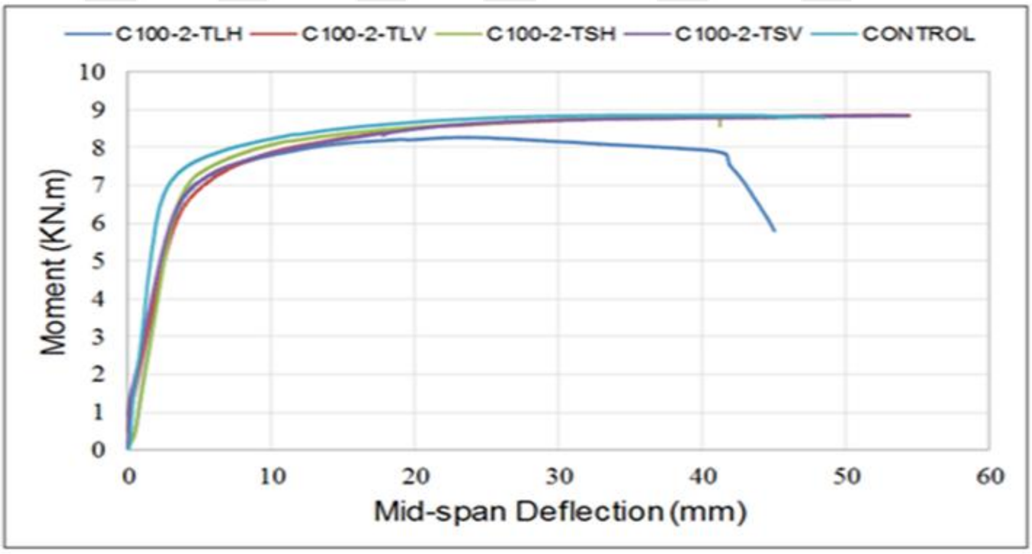

Figure 4.14 Moment capacity and mid span deflection for group four.

The fifth group (BLV, BLH, BSV and BSH) in this group the notch was at the bottom where the vertical notch failure velocity more than the horizontal notch, in which case the behavior of the four models was different from the control.

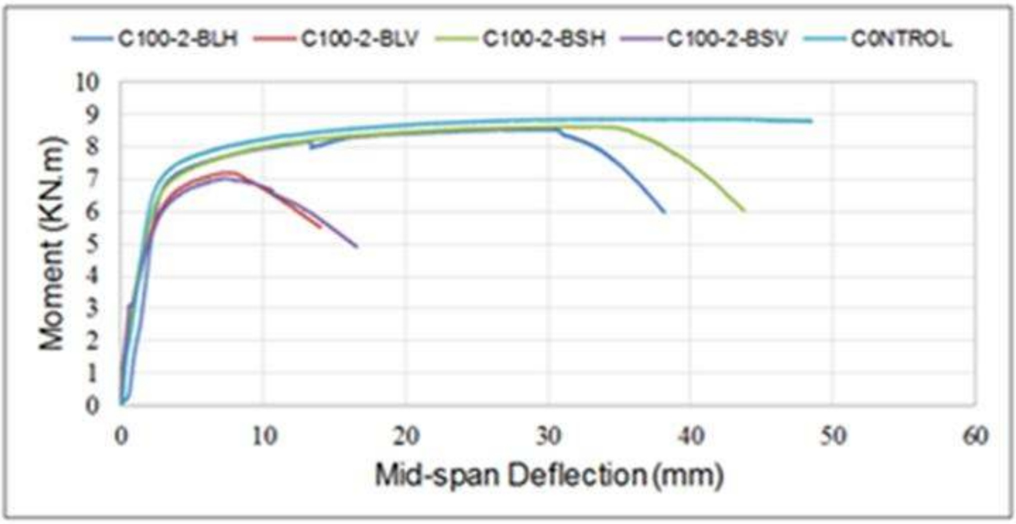

Figure 4.15 Moment capacity and mid span deflection for group five.

The sixth group (SLV, SLH, SSV and SSH) in this group was notch in the side where the models showed that vertical notch had a different behavior from the control so that it reached the failure stage in a little time while the models containing the horizontal notch had their behavior close to the control where they took more time to reach the failure stage.

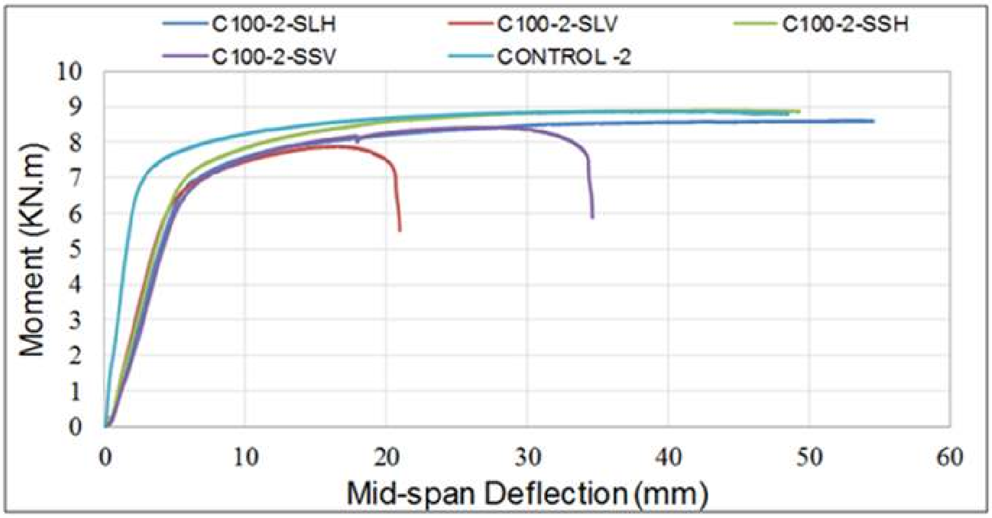

Figure 4.16 Moment capacity and mid span deflection for group six.

3.5 Moment capacities

The maximum experimental bending moments (Mu) for all beam specimens in all groups and percentage of increase in moment capacity of the notch beams compared to the control beams are tabulated in Table 4.1

For group one the percentage increase in the ultimate moment due to the notch beams were ranged from 5.7% for specimen C100-4-TLH to 0.74% for specimen C100-4-TLV to 0.09% for specimen C100-4-TSH to 0.08% for specimen C100-4-TSV. The results of the first group show that the model containing notch horizontal length of 5 cm has been affected more than the rest of the models compared to the control. As for the models C100-4-TLV.C100-4-TSV.C100-4-TSH, the decrease in moment ratio was close and close to the control.

For group two, the percentage increase in the ultimate moment due to the notch beams were ranged from 2.29% for specimen C100-4-BLH to 33.68% for specimen C100-4-BLV to 0.25% for specimen C100-4-BSH to 16.34% for specimen C100-4-BSV. This group shows a significant effect of decrease in moment in the C100-4-BLV model compared with the control. Next comes the model C100-4-BSV. This shows that the vertical notch effect bigger than of the horizontal notch effect at the bottom compare with the control.

For group three, the percentage increase in the ultimate moment due to the notch beams were ranged from 2.47% for specimen C100-4-SLH to 8.75% for specimen C100-4-SLV to 3.13% for specimen C100-4-SSH to 3.88% for specimen C100-4-SSV. In this group, the decrease in moment was high in the C100-4-SLV model compared to the control, while in the models C100-4-SLV and C100-4-SSH the ratio was not large between the two previous models. While the lowest effect was in the C100- 4-SSV compared to the control.

Table 4.1 Effect of moment on the beams 4mm.

Group name	Designation of beams	Moment. (kN.m)	% decrease in Moment. (kN.m)
	Control-4mm	16.29	----
GROUP ONE	C100-4-TLH	15.36	5.70
	C100-4-TLV	16.37	0.47
	C100-4-TSH	16.27	0.09
	C100-4-TSV	16.30	0.08
Group two	C100-4-BLH	15.92	2.29
	C100-4-BLV	10.80	33.68
	C100-4-BSH	16.25	0.25
	C100-4-BHV	13.63	16.34
Group three	C100-4-SLH	15.89	2.47
	C100-4-SLV	14.89	8.57
	C100-4-SSH	15.78	3.13
	C100-4-SSV	15.66	3.88

For group four the percentage increase in the ultimate moment due to the notch beams were ranged from 6.63% for specimen C100-2-TLH to 0.04% for specimen C100-2-TLV to 0.66% for specimen C100-2-TSH to 0.21% for specimen C100-2-TSV. In this group, the decrease in moment was high in the C100-2-TLH model, while in the models C100-2-TSH and C100-2-TSV, the ratio was not large between the two previous models. The lowest effect in the C100- 2-TLV compared to the control.

For group five the percentage increase in the ultimate moment due to the notch beams were ranged from 3.65% for specimen C100-2-BLH to 18.78% for specimen C100-2-BLV to 2.67% for specimen C100-2-BSH to 20.79% for specimen C100-2-BSV. In this group, the decrease in moment was high in the C100-2-BSV model and was high in the C100-2-BLV model, while in the C100-2-BLH model it was relatively low, while the model was not significant between the two models. While the least effect was in the C100-2-BSH model compared with the control. For group six the percentage increase in the ultimate moment due to the notch beams were ranged from 2.86% for specimen C100-2-SLH to 11.09% for specimen C100-2-SLV to 0.47 for specimen C100-2-SSH to 5.05% for specimen C100-2-SSV. In this group, the decrease in moment was high in the C100-2-SLV model and the ratio was lower in the C100-2-SSV model, while in the C100-2-SLH model it was relatively low while the least effect was in the C100-2-SSH model compared with the control.

When comparing the vertical notch long and short (5 cm and 2.5 cm) and its location top we find that the effect is small on the model as it was closed when the model reached the stage of failure. When comparing the vertical notch long and short (5 cm and 2.5 cm) and its position at the bottom we find that the effect is large and clear on the model where it was torn from one end when the model reached the stage of failure. When comparing vertical notch long and short (5 cm and 2.5 cm) was located in the side shows us that the effect of more than the top and less than the bottom in the model where it was rupture towards the bottom of one end when the model reached the stage of failure. The vertical notch is more influential at the bottom of the model. The long vertical incision is double the impact of the short vertical incision in the model. Well notch had a vertical effect when it was clearly on the side but lower than the bottom. When compared to the long and short horizontal notch (5 cm and 2.5 cm) and its location top us find that the notch long horizontal effect is more than notch Short horizontal when the model reached the stage of failure where the effect was more than notch vertical. When comparing the long and short notch (5 cm and 2.5 cm) and its position at the bottom find that the notch long horizontal effect is more than notch Short horizontal when the model reached the stage of failure but its effect was less than notch vertical. When comparing notch with long and short horizontal (5 cm and 2.5 cm) and its location in the side shows us that the notch long horizontal effect is more than notch Short horizontal when the model reached the stage of failure but its effect is much less than vertical notch. Conclusion of the past results shows us that notch vertical (long and short) has a greater impact than horizontal notch (long and short) and that the failure in vertical notch in the side or bottom is ruptured either at the top closing of notch vertical only. The notch horizontal was the case of failure when local twisting if it is on top either if it is at the bottom or side where it is closed.

Table 4.2 Effect of moment on the beams 2mm.

Group name	Designation of beams	Moment.(kN.m)	% decrease in Moment. (kN.m)
Group four	CONTROL-2mm	8.87	-----
	C100-2-TLH	8.28	6.63
	C100-2-TLV	8.86	0.04
	C100-2-TSH	8.81	0.66
	C100-2-TSV	8.85	0.21
Group five	C100-2-BLH	8.54	3.65
	C100-2-BLV	7.20	18.78
	C100-2-BSH	8.63	2.67
	C100-2-BSV	7.02	20.79
Group six	C100-2-SLH	8.61	2.86
	C100-2-SLV	7.88	11.09
	C100-2-SSH	8.91	0.47
	C100-2-SSV	8.42	5.05

3.6 Ductility

Ductility is the ability of material to undergo permanent deformation through elongation, also, to withstand plastic deformation and to bend without rupture. The ductility index of strengthening CFST beams had been determined for all groups as shown in Table 4.3 and Table 4.4 The ductility index (DI=Du/Dy) which represents the ratio of mid span deflection (Du) at ultimate moment (Mu) to the mid span deflection (Dy) at M = 0.6Mu, was used to predict and compare the ductility of the notch beams compared to the control specimens. According to the obtained results for group one, the Ductility Index (DI) ranged from 7.04 for specimen C100-4-TLH to 11.5 for specimen C100-4-TSH to 16.42 for specimen C100-4-TLV to 17.42 for specimen C100-4-TSV. Obviously, the maximum of DI obtained for the first set package is 17.42 for sample C100-4-TSV. The DI limit for the sample C100-4-TLV is 16.42, and the corresponding DI pack is 14.12, so that the control beam is less flexible than the beams CFST- Vertical notch in this group.

According to the obtained results for group two, the (DI) ranged from 5.82 for specimen C100-4-BLH to 15.61 for specimen C100-4-BSH to 4.01 for specimen C100-4-BSV to 4.93 for specimen C100-4-BLV. It is clear that the maximum of DI obtained for the second group is 15.61 for sample C100-4-BSH, and the corresponding control pack DI is 14.12, so that the control beam is less flexible than the models in this group. For group three, the Ductility C100-4-SSH to 8.38 for specimen C100-4-SLV to 12.06 for specimen C100-4-SSV. It is clear that the maximum DI obtained for the third group is 12.06 for sample C100-4-SSV, and the corresponding control pack DI is 14.12, so that the control beam is more flexible than this model in this group. For group four, the (DI) ranged from 9.22 for specimen C100-2-TLH to 15.39 for specimen C100-2-TSH to 19.20 for specimen C100-2-TLV to 21.75 for specimen C100-2-TSV. It is clear that the maximum of DI obtained for the fourth group is 21.75 for sample C100-2-TSV, and the corresponding control package DI is 24.43, so that the control beam is more flexible than this model in this group. For group five, the (DI) ranged from 13.76 for specimen C100-2-BLH to 18.01 for specimen C100-2-BSH to 4.95 for specimen C100-2-BLV to 5.05 for specimen C100-2-BSV. It is clear that the maximum of the DI obtained for the fifth group is 18.01 for sample C100-2-BSH, and the corresponding control package DI is 24.43, so that the control beam is more flexible than this model in this group. For group six, the (DI) ranged from 33.94 for specimen C100-2-SLH to 14.69 for specimen C100-2-SSH to 4.97 for specimen C100-2-SLV to 8.11 for specimen C100-2-SSV. It is clear that the maximum of DI obtained for group six is 33.94 for sample C100-2-SLH, and the corresponding control DI is 24.43, so that the control beam is less flexible than this model in this group.

Table 4.3 Ductility Index (DI) on the beams 4mm.

No	Specimen	Mid span deflection Du. at Mu. (mm)	Mid span deflection Du. at (0.6Mu) (mm)	Ductility index Du / Du(0.6Mu)
	S100-4- Control	36.06	2.55	14.12
Group one	C100-4-TLH	19.92	2.83	7.04
	C100-4-TSH	33.57	2.91	11.55
	C100-4-TLV	47.01	2.86	16.42
	C100-4-TSV	41.96	2.41	17.42
Group two	C100-4-BLH	15.91	2.73	5.82
	C100-4-BSH	37.67	2.41	15.61
	C100-4-BLV	9.11	2.27	4.01
	C100-4-BSV	14.10	2.86	4.93
Group three	C100-4-SLH	27.34	2.73	10.01
	C100-4-SSH	28.77	2.64	10.88
	C100-4-SLV	19.99	2.39	8.38
	C100-4-SSV	34.34	2.85	12.06

Table 4.4 Ductility Index (DI) on the beams 2mm.

No	Specimen	Mid span deflection Du. at Mu. (mm)	Mid span deflection Du. at (0.6Mu) (mm)	Ductility index Du / Du(0.6Mu)
	C100-2- Control	41.52	1.70	24.43
Group four	C100-2-TLH	23.22	2.52	9.22
	C100-2-TSH	41.26	2.68	15.39
	C100-2-TLV	53.04	2.76	19.20
	C100-2-TSV	53.18	2.47	21.57
Group five	C100-2-BLH	28.49	2.08	13.67
	C100-2-BSH	31.79	1.76	18.11
	C100-2-BLV	7.46	1.51	4.95
	C100-2-BSV	7.28	1.44	5.05
Group six	C100-2-SLH	53.09	1.59	33.49
	C100-2-SSH	44.07	3.00	14.69
	C100-2-SLV	16.53	3.33	4.97
	C100-2-SSV	22.31	2.75	8.11

CHAPTER 5

CONCLUSION AND RECOMNDSTION

5.1 Conclusions

In this study, the results of an experimental study to investigate the effect the notch in performance of concrete-filled steel tube beams. based on the experimental results, the following conclusions can be indicated;

- All the beams showed a smooth moment deflection curve with large deflection up to failure. The control beams have keep their maximum flexural capacity. It was found that the concrete inside the tubes have significantly increase the moment carrying capacity, stiffness and ductility.

- The control beams showed elastic behavior at the first stage of loading. Then, the curves follow an inelastic path with decreasing stiffness until reaching the maximum bending capacity.

- At the end of the test the control failed by bending stress and notch in bottom beams failed by rupture of bottom tension flange at almost the same maximum deflection capacity for beams. As obtained in the C100-4-BLV sample of the first group. In addition, sample C100-4-BSV from the second group. As well as C100-2-BLV and sample C100-2-BSV from the fifth group In contrast, notch in top beams failed by local buckling as obtained in sample C100-4-TLH of the first group In addition, sample C100-2-TLH from the fourth group and the closure of the notch if it is vertically. However, notch in side beams failed by rupture in the case of vertical notch. In addition, the closure of the notch if it is horizontal.

- Maximum deflection capacity at the end of the test compared to the control beams. Group one the DI limit for the sample C100-4-TLV is 16.42, and the corresponding DI value is 14.12. Group two it is clear that the maximum of DI obtained for the second group is 15.61 for sample C100-4-BSH.

- So that the control beam is less flexible than the two models. Also for group six is 33.94 for sample C100-2-SLH, and the corresponding control DI is 24.43, so that the control beam is less flexible than this model in this group.

- The effect of the vertical notch is more obvious than the horizontal notch. Therefore, the long and short vertical notch is more dangerous to the beams than the horizontal notch, especially if it is at the bottom it leads to rupture and different directions.

- Vertical notch at the top is less dangerous than the horizontal notch beams. The notch does not have a local buckling.

- Vertical notch in the side is more dangerous to the beams than the horizontal notch. The notch vertical does not cause ruptures towards the bottom.

5.2 Recommendations for future research

In view of the above literature, it can be conducted that there is limited research in the field of CFST beam with the notch. Furthermore, up to the best knowledge of the authors, no any previous study was carried out on the CFST beam with the notch. So that the research in this field is still in the primary stage and more efforts are required to fill this gap in the literature. This study included a test different thickness of the tube (2mm, 4mm) containing industrial notches. In addition, the notches are different directions (V, H) and different dimensions (L, S), in three different locations (T, B, S) also investigating the flexural performance of Self-Compacting Concrete (SCC) filled steel tube beams, and through this study, we conclude the effect of the notch. for all the point above the notch in the bottom more effect and danger to the structures when compare with the notch top and sidewall for (2 mm,4 mm) in addition to the notch in the bottom had less than ductility from top and sidewall for (2mm,4mm). There is still a wide range of CFST beams with notch and different thickness to use in future research. This will the risk ratio is determined and reduced. Besides circular tube, situations may arise in practical applications to use another shape tube. Thus, additional research is necessary to understand the behavior of notch on the CFST beam with different shape of tube section

`

REFERENCES

Donnell LH, Wan CC (1950). Effect of imperfections on buckling of thin cylinders and columns under axial compression. *Journal of Applied Mechanics: ASME;* **17(1)**:73–83.

J.F. Jullien, A. Limam (1998). Effects of openings of the buckling of cylindrical shells subjected to axial compression. *Thin-Walled Structures*, **31**, 187-202

Kuo-long LEE, Chien-min HSU, Wen-fung PAN (2014). Response of sharp-notched circular tubes under bending creep and relaxation. *Mechanical Engineering Journal,* 2.

Xu Chang, Lei Fu, Hong-Bo Zhao, Yong-Bin Zhang (2013). Behaviors of axially loaded circular concrete-filled steel tube (CFT) stub columns with notch in steel tubes. *Thin-Walled Structures*, **73**. 273–280.

Al-Amery, R., Al-Mahaidi, R. (2006). Coupled flexural–shear retrofitting of RC beams using CFRP straps, *Composite Structures*, **75(1)**, 457-464.

Alfawakhiri, F. (1997). Behavior of high-strength concrete-filled circular steel tube beam-columns, *University of Ottawa (Canada).*

X. Chang, X.L. Luo, C.X. Zhu, et al.,) (2014). Analysis of circular concrete-filled steel tubesupport in high ground stress conditions, *Tunn. Undergr. Space Technol.* **43** (641–48).

Han L-H, Yao G-H, Zhao X-L (2005). Tests and calculations for hollow structural steel (HSS) stub columns filled with self-consolidating concrete (SCC). *Journal of Constructional Steel Research*; **61(9)**,1241–69.

Tutuncu, (2001). Compressive Load and Buckling Response of Steel Pipelines during Earthquakes (Ph.D. thesis*), Cornell University, Ithaca, N.Y*

L.H. Donnell, C.C. Wan, (1950). Effect of imperfections on buckling of thin cylinders and columns under axial compression, *J. Appl. Mech.: ASME* ***17*** **(1)**, 325–348.

C. Edmundo, P.V. Suhas, (1996). Buckling of elastic-plastic square tubes under bending, *Int. J. Mech. Sci*. **38** **(7)**, 753–775.

`

C. Edmundo, P.V. Suhas, (1996). Buckling of elastic-plastic square tubes under bending, *Int.J. Mech. Sci*. **38 (7)**, 753–775.

Y. Liu, B. Young, (2003). Buckling of stainless-steel square hollow section compression members, *J. Constr. Steel Res*. **59 (4)**, 165–177.

O. Jensen, M. Langseth, O.S. Hopperstad, (2004). Experimental investigations on the behavior of short to long square aluminum tubes subjected to axial loading, *Int. J.Impact Eng*., **30 (7–8)**, 973–1003.

C.J. Stull, J.M. Nichols, (2011) Earls. Stochastic inverse identification of geometric imperfections in shell structures, *Comput. Methods Appl. Mech. Eng. **198*** **(25–28)** 2256–2267.

Alavi Nia, K.H. Fallah Nejad, H. Badnava, et al. (2012). Effects of buckling initiators on mechanical behavior of thin-walled square tubes subjected to oblique loading, *Thin-Walled Struct*. **59 (10)** 87–96.

Z. Sadovsky, J. Krivacek, V. lvanco, et al. (2012). Computational modelling of geometric imperfections and buckling strength of cold-formed steel, *J. Constr. Steel Res,*. **78 (11)**, 1–7.

X.W. Zhang, H. Su, T.X. Yu (2009). Energy absorption of an axially crushed square tube with a buckling initiator, *Int. J. Impact Eng*., **36 (3)**, 402–417.

Alavi Nia, H. Badnava, K.H. Fallah Nejad, (2011). An experimental investigation on crack effect on the mechanical behavior and energy absorption of *thin-walled tubes,Mater*. Des., **32 (6)**, 3594–3607.

L.H. Han, C. Hou, Q.L. Wang, (2012). Square concrete filled steel tubular (CFST) members under loading and chloride corrosion: experiments, *J. Constr. Steel Res.,* **71 (12),** 11–25.

H.E. Estekanchi, A. Vafai, (1999). On the buckling of cylindrical shells with through cracks under axial loading, *Thin-Walled Struct*., **35 (4),** 255–274.

Vafai, H.E. Estekanchi, (2006). Buckling of cracked cylindrical thin shells under combined internal pressure and axial compression, *thin-Walled Struct*., **44 (2),** 141–151.

J.F. Jullien, A. Limam, (2004). Effects of openings of the buckling of cylindrical shells subjected to axial compression, *Thin-Walled Struct*. **31 (1–3),** 79–99.

V. Papadopoulos, M. Papadrakakis, (2005). The effect of material and thickness variability on the buckling load of shells with random initial imperfections, *Comput. Methods Appl. Mech. Eng*. **194 (12–16)**, 1405–1426.

V. Papadopoulos, I. Pavols, (2007). The effect of non-uniformity of axial loading on thebuckling behavior of shells with random imperfections, *Int. J. Solid Struct.* **44 (1819)**, 6299–6317.

V. Papadopoulos, G. Stefanou, (2009). Buckling analysis of imperfect shells with stochastic non-Gaussian material and thickness properties, *Int. J. Solid Struct*., **46 (14–15),** 6299–6317.

Z. Tao, B. Uy, F.Y. Liao, et al., (2006). Nonlinear analysis of concrete-filled square stainless-steel stub columns under axial compression, *J. Constr. Steel Res*., **67 (11)** 1719–1732.

X. Chang, L. Fu, H.B. Zhao, et al., (2013). Behaviors of axially loaded circular concrete-filled steel tube (CFT) stub columns with notch in steel tubes, *Thin-walled Struct*. **73 (12),** 273–280.

Al-Zand, A. W., Badaruzzaman, W. H. W., Mutalib, A. A., & Hilo, S. J. (2014). Finite element analysis of concrete-filled steel tube beams partially wrapped with CFRP sheet, *International Journal of Technical Research and Applications*, 04-08.

Ammari, M. Z., Al-Nasra, M. M., & Najmi, A. (2013). Effective use of U-Link in Concrete Filled Steel Tubes Beams, *International Journal of Engineering Science Invention*, 2, 59-66.

Anjali M. S. and Eapen Sakaria (2015). Retrofitting of concrete filled cold formed steel tubular beams with GFRP sheets: experimental investigation, *International Journal of Innovative Research in Science, Engineering and Technology,* **4.**

Arivalagan, S., Kandasamy, S. (2010). Flexural and cyclic behavior of hollow and concrete-filled steel tubes.

Ashraf A. A. (2014). Strengthening of R.C. beams by external steel plate using mechanical connection technique, *Journal of Engineering and Development*, **18**.

Aykac, S., Kalkan, I., Aykac, B., Karahan, S., & Kayar, S. (2012). Strengthening and repair of reinforced concrete beams using external steel plates, *Journal of Structural Engineering*, **139(6)**, 929-939.

Barnes, R. A., Baglin, P. S., Mays, G. C., & Subedi, N. K. (2001). External steel plate systems for the shear strengthening of reinforced concrete beams, *engineering structures*, **23(9)**, 1162-1176.

Buyukozturk, O., & Hearing, B. (1998). Failure behavior of precracked concrete beams retrofitted with FRP, *Journal of composites for construction*, **2(3)**, 138-144.

Charif, A. (1983). Structural behavior of reinforced concrete beams strengthened by epoxy bonded steel plates *(Doctoral dissertation, University of Sheffield).*

Chitawadagi, M. V., Narasimhan, M. C. (2009). Strength deformation behavior of circular concrete filled steel tubes subjected to pure bending, *Journal of constructional steel research*, **65(8)**, 1836-1845.

Elchalakani, M., Zhao, X. L., Grzebieta, R. (2004). Concrete-filled steel circular tubes subjected to constant amplitude cyclic pure bending, *Engineering structures*, **26(14)**, 2125-2135.

Elchalakani, M., Zhao, X. L., Grzebieta, R. H. (2001). Concrete-filled circular steel tubes subjected to pure bending, *Journal of Constructional Steel Research*, **57(11)**, 1141-1168.

Fanning, P. J., Kelly, O. (2001). Ultimate response of RC beams strengthened with CFRP plates, *Journal of Composites for Construction*, **5(2)**, 122-127.

Garden, H. N., Hollaway, L. C. (1998). An experimental study of the influence of plate end anchorage of carbon fiber composite plates used to strengthen reinforced concrete beams, *Composite Structures*, **42(2)**, 175-188.

Ghannam, S. (2016). Flexural strength of concrete-filled steel tubular beam with partial replacement of coarse aggregate by granite, *International Journal of Civil Engineering and Technology (IJCIET)*, **7**, 161-168.

Han, L. H. (2004). Flexural behavior of concrete-filled steel tubes, *Journal of Constructional Steel Research*, **60(2)**, 313-337.

Han, L. H., Li, W., Bjorhovde, R. (2014). Developments and advanced applications of concrete-filled steel tubular (CFST) structures: members, *Journal of Constructional Steel Research*, **100**, 211-228.

Han, L. H., Lu, H., Yao, G. H., Liao, F. Y. (2006). Further study on the flexural behaviour of concrete-filled steel tubes, *Journal of Constructional Steel Research*, **62(6)**, 554-565.

Khalifa, A., Nanni, A. (2002). Rehabilitation of rectangular simply supported RC beams with shear deficiencies using CFRP composites, *Construction and building materials*, **16(3)**, 135-146.

Kiruthika, P., Balasubramanian, S., Sundarraja, M. C., Jegan, J. (2015). Strengthening of Cncrete Filled Steel Tubular Columns using FRP Composites, *International Journal of Innovative Research in Science, Engineering and Technology*, **4(4)**.

Kvedaras, A. K., Šaučiuvėnas, G., Komka, A., Jarmolajeva, E. (2013). Analysis of behaviour for concrete-filled steel tubular beams, *Advances in Structural Engineering and Mechanics*.

Lai, Z. (2014). Experimental database, analysis and design of noncom pact and slender concrete-filled steel tube (CFT) members.

Lai, Z., Varma, A. H. (2015). Non-compact and slender circular CFT members: Experimental database, analysis, and design, *Journal of Constructional Steel Research*, **106**, 220-233.

Lai, Z., Varma, A. H., Zhang, K. (2014). Non-compact and slender rectangular CFT members: Experimental database, analysis, and design, *Journal of Constructional Steel Research*, **101**, 455-468.

Leung, C. K. (2001). Delamination failure in concrete beams retrofitted with a bonded plate, *Journal of Materials in Civil Engineering*, 13(2), 106-113.

Li, W., Han, L. H., Chan, T. M. (2015). Performance of concrete-filled steel tubes subjected to eccentric tension, *Journal of Structural Engineering*, **141(12)**.

Mohanraj, E. K., Kandasamy, S., Raja Raman, A. (2010). Seismic behavior of concrete filled steel tubular beams, *In 35th Conference on Our World in Concrete & Structures* (25-27).

Mohiuddin, K., Ankara, R. (2016). Behavior of concrete-filled steel tubular beam with partial replacement of demolition waste as a coarse aggregate, *International Research Journal of Engineering and Technology*, **3(12)**, 218-222.

Morino, S., Tsuda, K. (2003). Design and construction of concrete-filled steel tube column system in Japan, *Earthquake Engineering and Engineering Seismology*, **4(1)**, 51-73.

Morsy, A., Mahmoud, E. T. (2013). Bonding techniques for flexural strengthening of RC beams using CFRP laminates, *Ain Shams Engineering journal*, **4(3)**, 369-374.

Nurbaiah, M. N., Hanizah, A. H., Nursafarina, A., Ashikin, M. N. (2010). Flexural behaviour of RC beams strengthened with externally bonded (EB) FRP sheets or Near Surface Mounted (NSM) FRP rods method, *In Science and Social Research (CSSR), 2010 International Conference on* (1232-1237). IEEE.

Obaidat, Y. T., Heyden, S., Dahlblom, O. (2010). The effect of CFRP and CFRP/concrete interface models when modelling retrofitted RC beams with FEM. *Composite Structures*, **92(6)**, 1391-1398.

Obaidat, Y. T., Heyden, S., Dahlblom, O., Abu-Farsakh, G., & Abdel-Jawad, Y. (2011). Retrofitting of reinforced concrete beams using composite laminates, *Construction and Building Materials*, **25(2)**, 591-597.

Oyawa, W. O., Sugiura, K., Watanabe, E. (2004). Flexural response of polymer concrete filled steel beams, *Construction and Building Materials*, **18(6)**, 367-376.

Qeshta, I. M., Shafigh, P., Jumaat, M. Z. (2015). Flexural behavior of RC beams strengthened with wire mesh-epoxy composite, *Construction and Building Materials*, **79**, 104-114.

Rahimi, H., Hutchinson, A. (2001). Concrete beams strengthened with externally bonded FRP plates, *Journal of composites for construction*, **5(1)**, 44-56.

Roeder, C. W., Lehman, D. E., Bishop, E. (2010). Strength and stiffness of circular concrete-filled tubes, *Journal of structural engineering*, **136(12)**, 1545-1553. 66

Sheikh, S. A. (2002). Performance of concrete structures retrofitted with fiber reinforced polymers, *engineering structures*, **24(7)**, 869-879.

Soundararajan, A., Shanmugasundaram, K. (2008). Flexural behavior of concrete filled steel hollow sections beams. *Journal of Civil Engineering and Management*, **14(2)**, 107-114.

Su, R. K. L., Zhu, Y. (2005). Experimental and numerical studies of external steel plate strengthened reinforced concrete coupling beams, *Engineering structures*, **27(10)**, 1537-1550.

Sundarraja, M., Prabhu, G. (2014). Experimental Investigation on Strengthening of CFST Members under Flexure Using CFRP Fabric, *Arabian Journal for Science & Engineering (Springer Science & Business Media BV),* **39(2)**, 659–668.

Täljsten, B. (1997). Strengthening of beams by plate bonding, *Journal of materials in civil engineering*, 9(4), 206-212.

Tao, Z., Han, L. H. (2006). Behavior of concrete-filled double skin rectangular steel tubular beam–columns, *Journal of Constructional Steel Research*, **62(7)**, 631-646.

Tao, Z., Han, L. H. (2007). Behavior of fire-exposed concrete-filled steel tubular beam columns repaired with CFRP wraps, *Thin-walled structures*, **45(1)**, 63-76.

Tao, Z., Han, L. H., Wang, L. L. (2007). Compressive and flexural behavior of CFRP-repaired concrete-filled steel tubes after exposure to fire, *Journal of Constructional Steel Research*, **63(8)**, 1116-1126.

Teng, J. G., Chen, J. F., Smith, S. T., & Lam, L. (2002). FRP: strengthened RC structures, *Frontiers in Physics*, 266.

Varma, A. H., Ricles, J. M., Sause, R., Lu, L. W. (2002). Seismic behavior and modeling of high-strength composite concrete-filled steel tube (CFT) beam–columns, *Journal of Constructional Steel Research*, **58(5)**, 725-758.

Vijay laxmi B. V. and Manoj Kumar Chitawadagi, (2014). Finite element analysis of concrete filled steel tube (cft's) subjected to flexure, *International Journal of Engineering Inventions*, 3, 18-28.

Wang, Z. B., Yu, Q., Tao, Z. (2015). Behaviour of CFRP externally-reinforced circular CFST members under combined tension and bending, *Journal of Constructional Steel Research*, **106**, 122-137.

Wu, Y. F., Griffith, M. C., Oehlers, D. J. (2003). Improving the strength and ductility of rectangular reinforced concrete columns through composite partial interaction: tests, *Journal of Structural Engineering*, **129(9)**, 1183-1190.

Wu, Y. F., Oehlers, D. J., Griffith, M. C. (2002). Partial-interaction analysis of composite beam/column members, *Mechanics of Structures and Machines*, **30(3)**, 309-332. 67

Wang, Y. (2006). Development of New CFT Column-CFT Beam Frame Structure using Self-compacting Concrete.

Zhou, M., Xu, L. Y., Tao, M. X., Fan, J. S., Hajjar, J. F., Nie, J. G. (2017). Experimental study on confining-strengthening, confining-stiffening, and fractal cracking of circular concrete filled steel tubes under axial tension, *Engineering Structures*, **133**, 186-199.